J. Phys. B: At. Mol. Opt. Phys. **30** (1997) 5305–5315. Printed in the UK PII: S0953-4075(97)82630-2

Electron-impact study for the $3\,^1$S and $n\,^1$P ($n = 3$–6) excitations in helium

Z P Zhong, R F Feng, S L Wu, L F Zhu, X J Zhang and K Z Xu

Department of Modern Physics, University of Science and Technology of China, Hefei, Anhui, 230027, People's Republic of China

Received 17 March 1997, in final form 10 July 1997

Abstract. Differential cross sections and generalized oscillator strengths for the $3\,^1$S and $n\,^1$P ($n = 3$–6) excitations overlapping neighbour non-dipole excitations in helium have been measured by an angle-resolved electron energy loss spectrometer at an impact energy of 1500 eV in a scattering angular range of 1.0–6.0°. These data are first reported at such a high impact energy. Integral cross sections for the above $n\,^1$P ($n = 3$–6) excitations were also determined. Meanwhile, the absolute optical oscillator strength density spectrum in the valence region of helium was established at the same impact energy in a mean scattering angle of 0°, and the absolute optical oscillator strengths for these discrete transitions corresponding to the valence region of helium are reported. All these experimental results are compared with previous appropriate published data.

1. Introduction

Electron collisions with atoms play an important role as an elementary process in such fields as plasma physics, chemistry, gaseous discharge and laser development. Differential cross sections (DCSs) are useful in gaining insight into the details of the collision mechanism, for instance, DCSs reflect more clearly the characteristics of the interaction potential than the integral cross section (ICS) and they are more critically dependent than ICS on the target wavefunction and approximate method employed in the calculation. Furthermore DCSs are of practical importance in applications, especially when a spatial anisotropy is involved. It is known [1, 2] that the generalized oscillator strength (GOS), which is directly related to the initial-state and excited-state wavefunctions, is proportional to the DCS for sufficiently fast electrons within the non-relativistic first Born approximation (FBA), it can be shown in the following Bethe–Born formula [1, 2]:

$$f(K, E) = \frac{E}{2}\frac{p_0}{p_a}K^2\frac{\mathrm{d}\sigma}{\mathrm{d}\Omega}. \tag{1}$$

Here $f(K, E)$ and $\mathrm{d}\sigma/\mathrm{d}\Omega$ stand for the GOS and DCS, respectively. E and K are the energy loss and momentum transfer while p_0 and p_a are the incident and scattered electron momentum, respectively. All the quantities in equation (1) and the following equations are in atomic units, the atomic unit of energy is the Hartree. Equation (1) can be used as a definition of the apparent GOS, $f(K, E, E_0)$ (E_0 stands for the impact energy), when DCSs are measured at an impact energy of E_0 and replace $\mathrm{d}\sigma/\mathrm{d}\Omega$ on the right-hand side of equation (1), regardless of whether the FBA holds or not at this impact energy. Thus, the apparent GOS provides the possibility to quantify the magnitude of the deviation of

0953-4075/97/225305+11$19.50

experimental data from the FBA data. In this way, the influence of higher-order effects (in terms of the Born series) can be studied.

Helium is an abundant element, almost as abundant as hydrogen in the universe, and its differential cross sections can easily be carried out to high accuracy by experimental measurements and theoretical calculations, because it is fairly easy to handle in experiments and is the simplest multi-electron atom in theoretical calculations. Therefore, absolute DCSs and GOSs of helium for electronic excitations are of undisputed interest in experimental measurements and theoretical calculations (see [3–8]). There are a large number of cross section calculations and measurements of helium, which have been summarized in [3–7]. In summary, so far there have been a few theoretical and experimental results for intermediate- or high-impact energy (more than 100 eV), a number of experimental ICS results but very limited experimental DCS results have been reported for the $n\,^1$S and $n\,^1$P excitations, especially for $n \geqslant 3$. In addition, most of these experimental and theoretical ICSs were obtained at impact energies E_0 lower than 1000 eV.

The purpose of this paper is to report experimentally derived absolute DCSs, GOSs and ICSs for the $3\,^1$S and $n\,^1$P ($n = 3$–6) excitations overlapping neighbouring non-dipole excitations of helium measured at an impact energy of 1500 eV in a scattering angular range of 1.0°–6.0°. These DCSs and GOSs are first reported at such a high impact energy. Integral cross sections for the unresolved $n\,^1$P ($n = 3$–6) excitations are also obtained. The absolute optical oscillator strength (OOS) density spectrum in the valence region of helium has also been determined at an impact energy of 1500 eV in a mean scattering angle of 0°.

2. Experimental apparatus and procedures

The electron energy loss spectrometer (EELS) used to obtain the data of helium in this work is an angle-resolved double-hemispherical EELS. Details of the apparatus were described in our previous work [9, 10]. Briefly it consists of an electron gun, a hemispherical electrostatic monochromator made of aluminium, a rotatable energy analyser of the same type, an interaction chamber, a number of cylindrical electrostatic optics lenses, and a channeltron for detecting the analysed electrons. All of these components are enclosed in four separate vacuum chambers made of stainless steel pumped by four turbomolecular pumps. Pulse-counting and multiscaler techniques were used in experimental measurements, which could record the corresponding counts at every measured energy-loss value, thus an energy-loss spectrum in which counts change with energy-loss value could be obtained. The impact energy of the spectrometer can be varied from 1 to 5 keV and the energy resolution is 40–120 meV (FWHM). The background pressure in the vacuum chambers was 3.0×10^{-5} Pa. The scattering angles were calibrated according to the symmetry of angular distribution for the inelastic scattering of the $1\,^1\text{S} \rightarrow 2\,^1$P of helium around the geometric nominal zero angle. The angular resolution of the spectrometer has been approximately determined from the angular distribution of the direct electron beam from the monochromator measured by rotating the analyser, and it is about 0.8° (FWHM) in the present measurements. The present energy scale was calibrated by using the discrete peak corresponding to the $2\,^1$P excitation of helium (21.218 eV). The impact energy was set at 1500 eV and the energy resolution was about 60 meV for the present measurements.

The present work is a continuation of [7], which reported the DCSs and GOSs for $2\,^1$P and $2\,^1$S excitations in helium using the same spectrometer with an energy resolution of 120 meV (FWHM) at an incident impact energy of 1500 eV. In order to eliminate the instability of the beam current and the variable scattering length seen by the energy analyser with different scattering angles, scattering intensities for the inelastic excitations

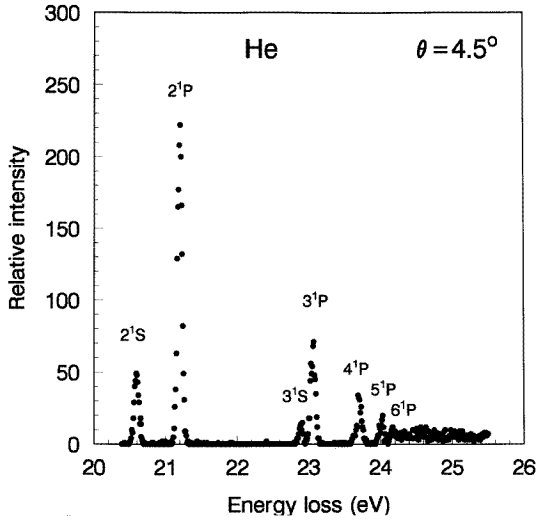

Figure 1. Electron energy loss spectrum for helium at an impact energy of 1500 eV and scattering angle of 4.5°.

associated with the $3\,^1$S and $n\,^1$P ($n = 3$–6) excitations were determined relative to the concurrent measured scattering intensities of the $2\,^1$P. These relative scattering intensities were obtained as the integrated counts under the individual spectral features from which a smooth and small background-scattering contribution was subtracted. We have measured these relative scattering intensity ratios at five different pressures: 0.008, 0.015, 0.020, 0.025 and 0.030 Pa. Xu *et al* [7] have shown that the correction of the pressure effect for the strongest $2\,^1$P peak was necessary only at those angles greater than 7°, in which the largest pressure used was 0.035 Pa. However, the present largest scattering angle was only 6.0°, thus the pressure effect in this work can be neglected. In fact, there was no significant pressure effect for the above transitions in this work. Figure 1 shows the present EELS spectrum in the valence region of helium at a scattering angle of 4.5° and a gas pressure of 0.020 Pa.

Absolute DCSs associated with the $3\,^1$S and $n\,^1$P($n = 3$–6) excitations have been determined by corresponding relative scattering intensities (with respect to the $2\,^1$P excitation) multiplying the corresponding absolute DCSs of the $2\,^1$P excitation, which has been obtained by the least-square fitted experimental data of Xu *et al* [7]. The final value of each DCS is an average over the measured results at the above five pressures. Corresponding absolute apparent GOSs have been obtained according to equation (1).

It can also be shown [1] that the generalized oscillator strength can be expanded in a power series of K^2 as

$$f(K, E) = f_o(E) + AK^2 + BK^4 + \cdots \tag{2}$$

where $f_o(E)$ is the OOS and A, B, etc are constants. Therefore, at the optical limit (i.e. $K^2 \to 0$), it will be found:

$$\lim_{K^2 \to 0} f(K, E) = f_o(E). \tag{3}$$

Lassettre *et al* [11] have conjectured, through some model and/or intuitive estimation that the apparent GOS at $K^2 \to 0$ is the OOS, regardless of whether the FBA holds or not,

i.e.

$$\lim_{K^2 \to 0} f(K, E, E_0) = f_o(E). \tag{4}$$

The conjecture is also called the theory of limiting oscillator strength. The following Lassettre formula [11] has been extensively used to determine an OOS by extrapolating apparent GOSs to $K^2 = 0$:

$$f(K, E, E_0) = \frac{1}{(1+y)^6}\left(f_o + \sum_{k=1}^{m} f_k \left(\frac{y}{1+y}\right)^k\right), \tag{5}$$

where $y = K^2/\alpha^2, \alpha = (2I)^{1/2} + [2(I-E)]^{1/2}$, and I is the ionization potential, f_o is the OOS and f_k are fitted constants which are related to E_0.

The absolute OOS for the $n\,^1$P (n = 3–6) excitation have been determined by extrapolating corresponding apparent GOSs to $K^2 = 0$ according to equation (5), which is called the extrapolating EELS method. The present fitting procedure is taken from [12].

The spectrometer used in the present work can be operated at a mean scattering angle of 0°, at which the optical limit (i.e. $K^2 \to 0$) is effectively satisfied when the impact energy is 1500 eV. In this work, the EELS spectrum was measured at an impact energy of 1500 eV (typical energy resolution of 60 meV (FWHM)), a mean scattering angle of 0° and a gas pressure of 0.004 Pa. The absolute OOS density spectrum was established by multiplying the Bethe–Born conversion factor of the spectrometer for the same experimental conditions and was normalized at 25.0 eV using the absolute value of Chan *et al* [13]. This is called the dipole (e, e) method and has been described in detail in [13]. Therefore, the OOS obtained by the two types of EELS methods can be compared with each other, and the theory of limiting oscillator strength [11] can be tested by comparing this work with previous results.

3. Results and discussions

3.1. Differential cross sections and generalized oscillator strengths

The experimental DCSs obtained in this work are listed in table 1. The average errors associated with the DCSs are given in parentheses. The statistical errors associated with the individual features and the errors specified for the DCSs of the $2\,^1$P excitation from [7] were

Table 1. Absolute differential cross sections for the $3\,^1$S and unresolved $n\,^1$P (n = 3–6) excitations (10^{-2} au).

Degree	$3\,^1$S	$3\,^1$P	$4\,^1$P	$5\,^1$P	$6\,^1$P
1.0	3.79 (0.60)	395.3 (28.8)	158.1 (11.4)	79.0 (5.4)	49.3 (3.2)
1.5	3.74 (0.44)	184.0 (13.6)	72.7 (5.3)	38.4 (2.7)	22.8 (1.6)
2.0	3.68 (0.29)	103.9 (7.3)	42.7 (3.0)	22.4 (1.6)	13.4 (1.6)
2.5	3.38 (0.27)	61.5 (4.3)	26.2 (1.9)	13.2 (1.0)	8.77 (1.09)
3.0	3.01 (0.25)	36.7 (2.6)	16.2 (1.2)	8.20 (0.62)	5.55 (0.71)
3.5	2.53 (0.21)	26.5 (1.9)	11.3 (0.8)	5.55 (0.43)	3.32 (0.43)
4.0	2.34 (0.20)	16.7 (1.2)	7.99 (0.60)	4.06 (0.32)	2.47 (0.32)
4.5	1.94 (0.17)	11.1 (0.8)	5.40 (0.41)	2.69 (0.22)	1.91 (0.26)
5.0	1.65 (0.13)	7.81 (0.58)	3.63 (0.28)	2.21 (0.18)	1.21 (0.17)
5.5	1.29 (0.11)	5.38 (0.40)	2.74 (0.22)	1.54 (0.13)	
6.0	1.02 (0.09)	3.57 (0.27)	2.08 (0.17)	1.16 (0.10)	0.567 (0.089)

considered. The total error was obtained as a square root of the sum of each contributing error square. The DCSs and apparent GOSs for the $n\,^1$P ($n = 3$–6) excitations include contributions of neighbouring non-dipole transitions. (The $3\,^1$P excitation includes the $3\,^{3,1}$P and $3\,^{3,1}$D excitations; the $4\,^1$P excitation includes the $4\,^{3,1}$S, $4\,^{3,1}$P, $4\,^{3,1}$D and $4\,^{3,1}$F excitations; the $5\,^1$P excitation includes the $5\,^{3,1}$S, $5\,^{3,1}$P, $5\,^{3,1}$D and $5\,^{3,1}$F excitations, etc; the $6\,^1$P excitation includes the $6\,^{3,1}$S, $6\,^{3,1}$P, $6\,^{3,1}$D and $6\,^{3,1}$F excitations, etc.) Contributions of these non-dipole transitions in the unresolved $n\,^1$P ($n = 3$–6) excitations can be estimated according to their ICS data at the same impact energy determined by Moussa *et al* [14] as follows. The ICS ratio of the $3\,^1$P excitation to the $3\,^{3,1}$P+$3\,^{3,1}$D excitations is approximately 99%, the one of the $4\,^1$P excitation to the $4\,^{3,1}$S+$4\,^{3,1}$P+$4\,^{3,1}$D excitations is approximately 90% and the one of the $5\,^1$P excitation to the $5\,^{3,1}$S+$5\,^{3,1}$P+$5\,^1$D excitations is approximately 90%. No available published data can be used to estimate the contribution of non-dipole transitions in the unresolved $6\,^1$P excitation. In sum, the present DCSs, apparent GOSs and ICSs for the unresolved $n\,^1$P ($n = 3$–6) excitations mainly arise from the corresponding dipole $n\,^1$P ($n = 3$–6) excitations.

So far there are no published experimental and theoretical data of DCSs for these excitations which can be compared with the present results. However, apparent GOSs at different impact energies can be compared with each other and with the ones predicted by the FBA. These comparisons shown in figures 2(*a*)–(*e*) are made among the present work, the FBA data and the previous data obtained at the impact energy of $E_0 \geqslant 100$ eV, because it is certain that the FBA method is not valid at very low impact energy.

For the $3\,^1$S excitation, available data are very limited. Appropriate experimental data are only reported by Trajmar *et al* [5] at the impact energy of 100 eV. Appropriate calculated data are from the FBA [15a, 16], the multichannel eikonal theory (MET) at 100 and 200 eV [17, 18], the distorted wave (DW) approximation at 100 eV [19], the distorted-wave polarized orbital (DWPO) method at 100 and 200 eV [20a], and the first-order form of the many-body theory (FOMBT) at 100 eV [5]. Most of these data and the present results are shown in figure 2(*a*) which clearly shows that the present data are in good agreement with the FBA data reported by Kim and Inokuti [15a]. However, other FBA data reported by Bell *et al* [16] are generally lower than our work and the FBA data of Kim and Inokuti [15a]. The present K^2 value corresponding to the maximum of the apparent GOS curve is 0.84 au, it is slightly smaller than the FBA data reported by Kim and Inokuti [15a], and Bell *et al* [16] (both corresponding K^2 are nearly 0.95 au). There are no other experimental data obtained at an impact energy larger than 100 eV. Differences in shape and magnitude for apparent GOSs between work reported in [5, 17, 20a] at 100 eV and our work are large, for example, there is a minimum for experimental [5] and theoretical data [17] near $K^2 = 0.3$ au except for the DWPO data [20a]. On the other hand, the shapes of calculated apparent GOS curves at 200 eV are similar to our work, they are close to our data at $K^2 \leqslant 0.3$ au although these apparent GOSs are much smaller than our results at $K^2 \geqslant 0.3$ au. There are too few data to accurately determine the position of the maximum at 200 eV.

For the $3\,^1$P excitation, it should be noted that so far there is no work for the resolved $3\,^1$P excitation in EELS. Most of the previous data are plotted in figure 2(*b*). Similar to the $3\,^1$S excitation, the present data for the unresolved $3\,^1$P excitation are also in good agreement with the FBA data reported by Kim and Inokuti [15a], and are different from the FBA data of Bell *et al* [16] in shape and magnitude. The data of Lassettre *et al* [21] were obtained at 511 eV from the overlap peaks of the $3\,^1$P and $4\,^1$P excitations. Thus it is not surprising that their data are generally larger than our values, but the shape of their apparent GOS curve is similar to ours. The experimental and FOMBT data in figure 2(*b*) reported by Cartwright

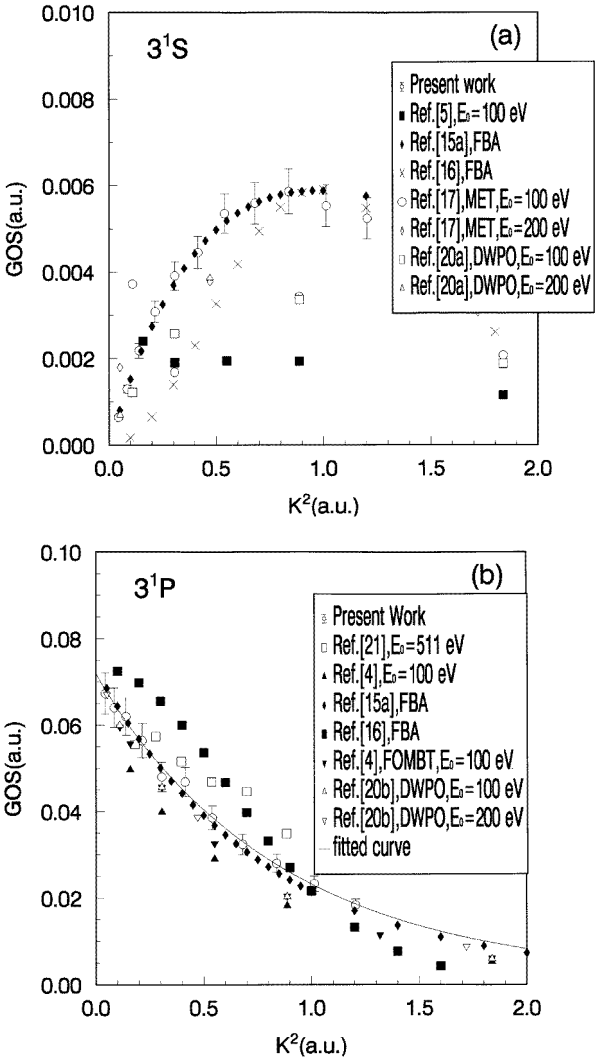

Figure 2. (*a*) Absolute GOSs for the $3\,^1$S as a function of K^2. (*b*) Absolute GOSs for the $3\,^1$P as a function of K^2, present results and the data of [4] include contributions of $3\,^{1,3}$D. (*c*) Absolute GOSs for the $4\,^1$P as a function of K^2, present results include contributions of neighbouring non-dipole transitions. (*d*) Absolute GOSs for the $5\,^1$P as a function of K^2, present results include contributions of neighbouring non-dipole transitions. (*e*) Absolute GOSs for the $6\,^1$P as a function of K^2, present results include contributions of neighbouring non-dipole transitions.

et al [4] at 100 eV are the sum of the $3\,^1$P, $3\,^1$D and $3\,^3$D excitations. Their values are smaller than ours, especially their experimental values. The calculated apparent GOSs at 100 and 200 eV [20b] are generally smaller than our data, but are consistent with ours within experimental errors. The shapes of all these apparent GOS curves (see figure 2(*b*)) are still similar to our work at an impact energy $E_0 \geqslant 100$ eV.

There are very limited experimental and calculated DCSs at any impact energy for the $4\,^1$P, $5\,^1$P and $6\,^1$P excitations. No available absolute experimental data can be compared with the present results for the above transitions. Only Le Nadan [22] has reported the

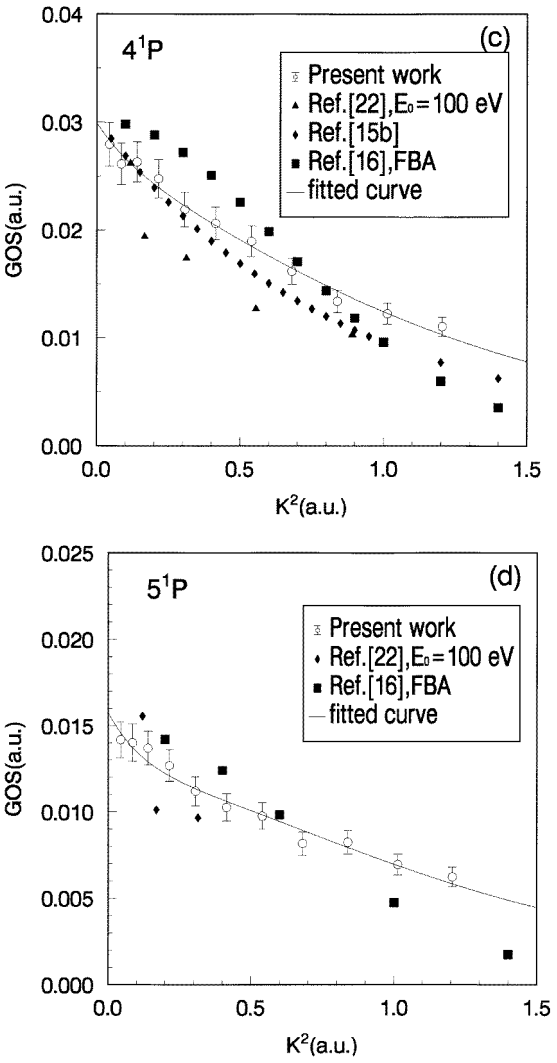

Figure 2. (Continued)

DCS ratios of the $4\,^1$P and $5\,^1$P excitations with respect to $2\,^1$P at 100 eV, which now are normalized using the absolute experimental DCSs (scattering angle is larger than 0°) and FOMBT data (scattering angle is 0°) of the $2\,^1$P excitation reported by Cartwright *et al* [4]. It clearly shows in figures 2(*c*) and (*d*) that the apparent GOSs of Le Nadan [22] for the $4\,^1$P and $5\,^1$P excitations are smaller than our results, but the differences between both data are similar to those in $3\,^1$P and the shape of the GOS curve for $4\,^1$P is similar to our work. The only available theoretical data for $n\,^1$P ($n = 4$–6) excitations are reported by Kim and Inokuti [15b], Bell *et al* [16] using the FBA method, it is evident from figures 2(*c*)–(*e*) that differences for the $n\,^1$P ($n = 4$–6) excitations in shape and magnitude between our work and the FBA data [16] are similar to those in the $3\,^1$P excitation. The calculated values for the $4\,^1$P excitation of Kim and Inokuti [15b] are consistent with the present results at $K^2 \leqslant 0.4$ au but they are lower than the present results at $K^2 \geqslant 0.4$ au, which may

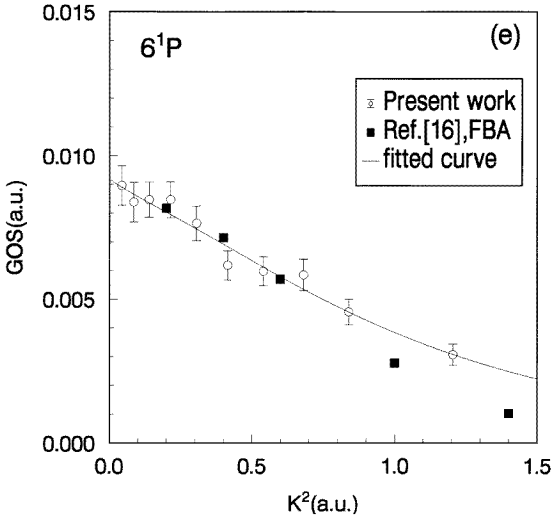

Figure 2. (Continued)

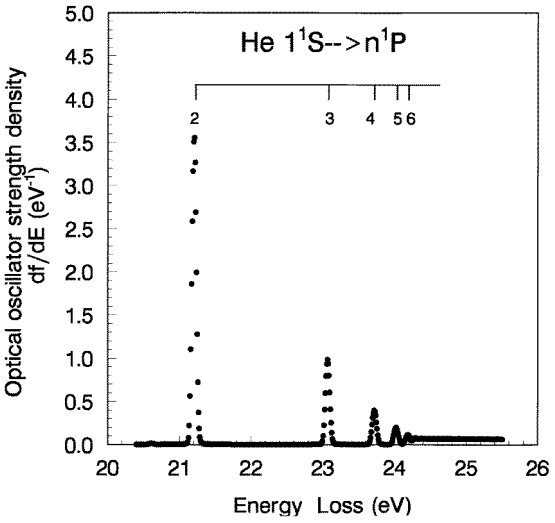

Figure 3. Absolute OOS density spectrum of helium in the valence range.

arise from the fact that the present data for the $4\,^1P$ excitation include the contribution of non-dipole transitions.

The comparison of the present data with the FBA data reported by Kim and Inokuti [15a], which have been experimentally verified for the $2\,^1S$ and $2\,^1P$ excitations at impact energies E_0 above 1500 eV (see Xu *et al* [7] and references therein) and can be regarded as accurate FBA results, establishes that the present apparent GOSs are equal to GOSs, thus, the present values obtained by equation (1) can be called GOSs.

Table 2. Absolute optical oscillator strengths for the $n\,^1$P ($n = 2$–6) excitations (au).

	$2\,^1$P	$3\,^1$P	$4\,^1$P	$5\,^1$P	$6\,^1$P
This work (dipole (e, e))	0.276	0.073 9	0.030 4	0.015 4	0.009 30
	(0.016)	(0.004 4)	(0.001 8)	(0.000 9)	(0.000 56)
This work (extrapolating EELS)		0.071 9	0.029 9	0.015 7	0.009 18
		(0.005 7)	(0.002 7)	(0.001 4)	(0.008 6)
[10] (dipole (e, e))	0.280	0.074 5	0.030 3	0.015 3	0.009 07
[13] (dipole (e, e))	0.280	0.074 1	0.030 3	0.015 2	0.008 92
[24] (optical method)	0.273	0.071			
[25] (optical method)	0.276	0.076	0.029 9		
[23] (theoretical)	0.276 17	0.073 43	0.029 861	0.015 039	0.008 627
[26] (theoretical)	0.281 1	0.074 34	0.030 28	0.015 24	0.008 734
[27] (theoretical)	0.276	0.073 4	0.029 9	0.015 1	0.008 6

3.2. Optical oscillator strengths

The present OOS density spectrum of helium in the valence region, which was obtained at an impact energy of 1500 eV and a mean scattering angle of 0°, is shown in figure 3. The OOSs for the $n\,^1$P ($n = 2$–6) excitations were determined by integrating counts under the individual spectral features. In addition, the present OOSs for the unresolved $n\,^1$P ($n = 3$–6) excitations obtained by the extrapolating EELS method are shown in figures 2(*b*)–(*e*). Table 2 only lists present OOSs obtained by the dipole (e, e) method and the extrapolating EELS method, the major previous experimental and theoretical OOSs summarized by Chan *et al* [13] through 1991 and recently published data reported by Feng *et al* [10] and Cann and Thakkar [23].

It has been shown [12] that the theory of limiting oscillator strength [11] holds for the vibronic bands of $A\,^1\Pi$, $C\,^1\Sigma^+$ and $E\,^1\Pi$ transitions of carbon monoxide, because their OOSs obtained by the two types of EELS methods are consistent with each other and agree reasonably with previous electron impact data. The present extrapolating OOSs for the $n\,^1$P ($n = 3$–6) excitations are also consistent with the corresponding present OOSs obtained by the dipole (e, e) method within experimental errors, and both of them agree well with the other OOSs of the dipole (e, e) method [10, 13], optical measurements [24, 25] and theoretical calculations [23, 26, 27] in table 2. That is, the theory of limiting oscillator strength [11] holds in the case of helium. Although the present extrapolating OOSs for the $n\,^1$P ($n = 3$–6) excitations were obtained through those GOSs of the unresolved $n\,^1$P ($n = 3$–6) excitations, the present extrapolating OOSs for the $n\,^1$P ($n = 3$–6) excitations are in good agreement with the other OOSs in table 2. Because the contributions of non-dipole transitions in the unresolved $n\,^1$P ($n = 3$–6) excitations are small, and the present GOSs were obtained at small scattering angles at which the contributions of non-dipole transitions are small. Therefore, the present GOSs for the unresolved $n\,^1$P ($n = 3$–6) excitations are mainly from the contributions of the dipole $n\,^1$P ($n = 3$–6) transitions.

3.3. Integral cross sections

Table 1 clearly shows that the DCSs for the unresolved $n\,^1$P ($n = 3$–6) excitations decrease dramatically with increasing scattering angles, thus the integral cross sections for the unresolved $n\,^1$P ($n = 3$–6) excitations are mainly from the contributions of DCSs at small

Table 3. Absolute integral cross sections for the $n\,^1$P ($n = 3$–6) excitations at an impact energy of 1500 eV (10^{-2} au).

	$3\,^1$P	$4\,^1$P	$5\,^1$P	$6\,^1$P
Experimental				
This work	2.08 (0.18)	0.869 (0.077)	0.445 (0.040)	0.268 (0.025)
[14]	1.953	0.8003	0.3909	
[30]	2.21	0.82		
[31]	2.13			
Theoretical				
[15a]	2.09			
[16]	2.09	0.839	0.420	0.239
[29]	2.35	1.01	0.458	0.263

scattering angles. Moreover, the ICS can be obtained as follows [28]:

$$\sigma(E_0) = \frac{2\pi}{EE_0}\int_{k_{\min}}^{k_{\max}} f(K, E, E_0)\frac{\mathrm{d}K}{K}. \tag{6}$$

In this way, the ICSs for the unresolved $n\,^1$P ($n = 3$–6) excitations can be obtained from the present fitted GOS curve according to equation (5). The present ratio of the sum of DCSs at scattering angles θ no more than 6.0° to the present ICS for the $3\,^1$P excitations is about 85%, therefore, the present ICS errors resulting from the larger scattering angle for the unresolved $n\,^1$P ($n = 3$–6) excitations are small.

The ICSs obtained from this work and all previous works at an impact energy of 1500 eV are listed in table 3. It should be noted that the data of Moussa *et al* [14] included the contribution of non-dipole transitions, and the data of Mityureva and Smirnov [29] were calculated using a three-parameter formula. The present ICSs for the unresolved $n\,^1$P ($n = 3$–5) excitations are generally larger than the experimental data of Moussa *et al* [14], by 6–12%, but their experimental error was 10% [14], therefore, the present values for the unresolved $n\,^1$P ($n = 3$–5) excitations agree reasonably well with their experimental data. The FBA data reported by Kim and Inokuti [15a] and Bell *et al* [16] also agree with the present data. The data of Mityureva and Smirnov [29] are generally larger than the present data by 3–13% except for the $6\,^1$P excitation. The other experimental data [30, 31] are consistent with the present data.

4. Conclusion

Absolute DCSs, GOSs for the $3\,^1$S and the unresolved $n\,^1$P ($n = 3$–6) excitations of helium have been first reported at an impact energy of 1500 eV and in a scattering angle range of 1.0–6.0°. The OOS density spectrum of helium in the valence range was also established at the impact energy of 1500 eV in a mean scattering angle of 0°. The optical oscillator strengths for the $n\,^1$P ($n = 2$–6) excitations have been determined by the dipole (e, e) method and extrapolating EELS method in this work. Extensive comparisons are made between available experimental and theoretical values. The present absolute apparent GOSs for the $3\,^1$S and $3\,^1$P excitations are in good agreement with the FBA results [15a]. In addition, the present OOS for $n\,^1$P ($n = 3$–6) obtained by the dipole (e, e) method and extrapolating EELS method are consistent with each other and with the previous works.

The present ICSs for the $n\,^1$P ($n = 3$–6) excitations are also consistent with the previous works.

Acknowledgments

The financial support for this work was provided by the National Natural Science Foundation of China and the National Education Committee of China. We also thank the University of Science and Technology of China for supporting this work.

References

[1] Bethe H 1930 *Ann. Phys.* **5** 325
[2] Inokuti M 1971 *Rev. Mod. Phys.* **43** 297
[3] Bransden B H and McDowell M R C 1977 *Phys. Rep.* **30** 207
Bransden B H and McDowell M R C 1978 *Phys. Rep.* **46** 249
[4] Cartwright D C, Csanak G, Trajmar S and Register D F 1992 *Phys. Rev.* A **45** 1602
[5] Trajmar S, Register D F, Cartwright D C and Csanak G 1992 *J. Phys. B: At. Mol. Opt. Phys.* **25** 4889
[6] Nakazaki S 1993 *Advances in Atomic, Molecular, and Optical Physics* vol 30 ed D Bates and B Bederson (New York: Academic) p 14
[7] Xu K Z, Feng R F, Wu S L, Ji Q, Zhang X J, Zhong Z P and Zheng Y 1996 *Phys. Rev.* A **53** 3081
[8] Wang J G, Tong X M and Li Jia-ming 1996 *Acta Phys. Sinica* **45** 13 (in Chinese)
[9] Wu S L, Zhong Z P, Feng R F, Xing S L, Yang B X and Xu K Z 1995 *Phys. Rev.* A **51** 4494
[10] Feng R F, Yang B X, Wu S L, Xing S L, Zhang F, Zhong Z P, Guo X Z and Xu K Z 1996 *Sci. China* A **39** 1288
[11] Lassettre E N, Skerbele A and Dillon M A 1969 *J. Chem. Phys.* **50** 1829
[12] Zhong Z P, Feng R F, Xu K Z, Wu S L, Zhu L F, Zhang X J, Ji Q and Shi C Q 1997 *Phys. Rev.* A **55** 1799
[13] Chan W F, Cooper G and Brion C E 1991 *Phys. Rev.* A **44** 186
[14] Moussa M H R, de Heer F J and Schutten J 1969 *Physica* **40** 517
[15a] Kim Y K and Inokuti M 1968 *Phys. Rev.* **175** 176
[15b] Kim Y K and Inokuti M 1969 *Phys. Rev.* **184** 38
[16] Bell K L, Kennedy D J and Kingston A E 1969 *J. Phys. B: At. Mol. Phys.* **2** 26
[17] Mansky E J and Flannery M R 1990 *J. Phys. B: At. Mol. Opt. Phys.* **23** 4573
[18] Flannery M R and McCann K J 1975 *J. Phys. B: At. Mol. Phys.* **8** 1716
[19] Katiyar A K and Srivastava R 1988 *Phys. Rev.* A **38** 2767
[20a] Scott T and McDowell M R C 1975 *J. Phys. B: At. Mol. Phys.* **8** 1851
[20b] Scott T and McDowell M R C 1976 *J. Phys. B: At. Mol. Phys.* **9** 2235
[21] Lassettre E N, Krasnow M E and Silverman S 1964 *J. Phys. Chem.* **40** 1242
[22] Le Nadan A 1970 *Thesis* Brest
[23] Cann N M and Thakkar A J 1992 *Phys. Rev.* A **46** 5397
[24] Tsurubuchi S, Watanabe S and Arikawa T 1989 *J. Phys. B: At. Mol. Opt. Phys.* **22** 2969
[25] de Jongh J P and Van Eck J 1971 *Physica* **51** 104
[26] Fernely J A, Taylor K T and Seaton M J 1987 *J. Phys. B: At. Mol. Phys.* **20** 6457
[27] Dalgarno A and Parkinson E M 1967 *Proc. R. Soc.* A **301** 253
[28] Vriens L 1967 *Phys. Rev.* **160** 100
[29] Mityureva A A and Smirnov V V 1993 *Opt. Spectrosc.* **74** 3
[30] Donaldson F G, Hender M A and McConkey J W 1972 *J. Phys. B: At. Mol. Phys.* **5** 1192
[31] Westervel W B, Heideman H G M and Van Eck J 1979 *J. Phys. B: At. Mol. Phys.* **12** 115